Matej Babič

Cristiano Fragassa[1]

Grzegorz Lesiuk

Dragan Marinković

A NEW METHOD FOR COMPLEXITY DETERMINATION BY USING FRACTALS AND ITS APPLICATIONS IN MATERIAL SURFACE CHARACTERISTICS

Abstract: In this article, a new method for complexity determination by using fractals in combination with an artificial intelligent approach is proposed and its application in laser hardening technology is detailed. In particular, nanoindentation tests were applied as a way to investigate the hardness properties of tool steel alloys with respect to both marginal and relevant changes in laser hardening parameters. Specifically, process duration and temperature were considered, together with nanoindentation, later related to surface characteristics by image analysis and Hurst exponent determination. Three different Machine Learning algorithms (Random Forest, Support Vector Machine and k-Nearest Neighbors) were used and predictions compared with measures in terms of mean, variability and linear correlation. Evidences confirmed the general applicability of this method, based on integrating fractals for microstructure analysis and machine learning for their deep understanding, in material science and process engineering.

*Keywords: Fractals; Complexity; Machine Learning; Laser Hardening; Surface Quality*

1. Introduction

In nature many geometrical structures and shapes, which are rather irregular, cannot be described with classical Euclidian geometry. Thus, a different approach for representing the complexity and the irregularity of those objects is needed. A modern and promising one is represented by fractals.

The term '*fractal*' was firstly coined in 1975 (Mandelbrot, 1977, 1983) to describe some mathematical situations that seemed to have a "chaotic" behavior, and derives from the Latin '*fractus*', equivalent to 'fractured'.

A fractal can be defined as a geometric object with an internal '*homothetia*': it is repeated in its form in the same way on different scales, and therefore enlarging any part of it, a figure similar to the original is obtained. Merging this object with similar ones, even simultaneously acting at different scales, new shapes and structures can be obtained (Figure 1).
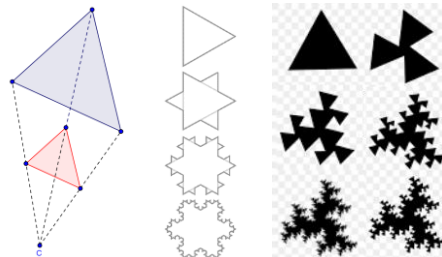
Figure 1. The concept of 'homothetia' in objects as base for building the fractal geometry

---

[1] Corresponding author: Cristiano Fragassa
Email: cristiano.fragassa@unibo.it

This concept of '**homothetia**' and the related fractal geometry was originally developed and used for the analysis of irregular features in nature reporting a large success. Besides, it has been also finding increasing applications in the fields of engineering and materials science. It is the case, for instance, of the characterization of microstructures (Smith et al., 2000; Martin, 2015) where fractals can explain their uncommon shape better than the Euclidian geometry. But fractal patterns were also observed in the computational mechanics of elastic-plastic transitions (Pande et al., 1987; Oswald & Vaughan, 2016) underlining the opportunity to consider them in predicting material properties (Mandelbrot et al., 1984).

Among the key concepts characterizing the fractal geometry, a special interest in this discussion is represented by the *fractal dimension* that can be considered as an index of the fractal complexity and, indirectly, of the geometrical irregularity of the related microstructure it can represent. Therefore, fractal dimensions has become a common practice for assessing material roughness, hardness or fracture surfaces (Kotowski, 2006; Kotowski et al., 2018). It also happens in the cases of material treatments, as robot laser hardening (*RLH*), where fractal geometry was conveniently used in the past, for instance, by Zhang et al., 2019.

Laser hardening probably represents the most convenient method for steel hardening nowadays (Chiang and Chen, 2005). This technology uses a flat semiconductor laser as a heat source and then employs this energy to perform a thermal treatment on the superficial layers of materials. It can operate with ferrous materials, including steel and cast iron, even in the presence of irregular parts. The metal workpieces, after being heated by the laser beam, are quickly cooled down in air (Figure 2).

Altering the zones, the laser, in brief, changes the relationship between stress (force / area) and strain (related proportional deformation) in a material, modifying its linear elasticity response, but also its plasticity behavior.

The positive effects of laser irradiation on metals and alloys is clearly highlighted in many investigations, as Bashir et al., 2013; Lin and Ren, 2014; Kazakevich et al., 2007.

The presence of **thermally altered zones** to a depth of several millimeters permits to improve material properties at surface as hardness and wear resistance. It is noteworthy that the process increases those properties in parts without melting the surface or breaking the geometrical continuity.

At the same time, since the heating period is quite short, in the case of laser technology deformation and surface oxidation in the altered zones are reduced compared to other treatments (Babu et al., 2012; Majumdar et al., 2009). Therefore, the use of laser beam in process technology can offer relevant advantages in manufacturing as a short wavelength that improves the surface quality, high efficiency in photoelectric conversion, low energy consumption and fewer efforts in parts refinishing permitting improvements in the overall process quality. In addition, it can be carried out under stationary conditions of process with evident benefits in productivity.
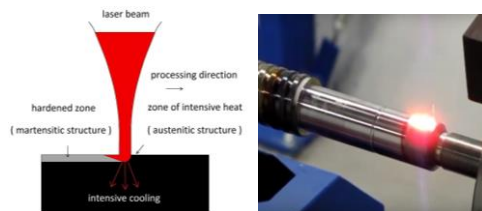
Figure 2. Laser hardening (*ks-kurim*)

In terms of metallurgy and micrographs, the surface hardness in the case of laser hardening in air was deeply related with the dislocation line density and the grain size effect by Naeem et al., 2019.

With the increase of thermal strain, the working hardening rate is on the rise uninterruptedly during tensile deformation before plastic collapse. This aspect was fully investigated in (Pang et al., 2019).

Other authors investigate the laser hardening in a special case. For instance, the effect of laser irradiation with different numbers of shots on the microstructure, the surface, and the mechanical properties of metal alloy were studied by scanning electron microscopy (*Di et al, 2009*; Babu et al., 2012). The influence of treatments on the bake hardening (BH) response in the case of an AlZnMgCuZr aluminium alloy used for automotive body structures were also analyzed.

These (and other) studies considered different process situations and technology aspects for the laser hardening showing that the treatment is characterized by a large number of factors such as, e.g., temperature distribution, cooling rate, thermal stress and so on.

Consequently, the effects of treatments in terms of changes in the material strengths have to be always balanced by other relevant features such as, e.g., process capability and sustainability. Proper optimisation is often necessary, and every consideration with this scope has to pass through the real possibility to predict the material properties with respect to changes in process parameters. Fractals can support this phase due to their capability to characterise information from microscopy.

Even if fractals can usefully represent structures of micrographs, they can hardly recognize the overall pattern.

It is noteworthy, in fact, that most of the fractals encountered in nature show a self-similarity that is generally random: they are not created by deterministic rules like for the Koch curve (von Koch, 1907). Thus, they are not exactly characterized by a self-similarity, rather than by a statistical self-affinity, implying that those objects exhibit self-similarity in some average sense and over a certain local range of length scales.

This inner simplicity, hidden behind the overall complexity given by the multiplicity of levels and scales, is one of the reasons why **Artificial Intelligence** (AI) could be really useful in decoding the hidden patterns.

Pattern Recognition can be considered as the science of 'making inferences from perceptual data', using methodological tools from statistics, probability, computational geometry, signal processes and algorithm design (Bishop, 2006). It is often applied in social sciences and finance, but also science and engineering nowadays. This is the case detailed in, e.g., Sang-Gyu et al., 2019 where patterns were recognized by surface images in the way to predict the process quality.

With this scope, **Machine Learning** (ML) is the additional concept regularly considered in combination with pattern recognition (Michel, 2014). ML represents a branch of Artificial Intelligence (AI) where the main idea is that the computer does not simply use a pre-written algorithm for its estimations but learns how to solve the problem by itself.

The good comparison between results offered by the AI and the ones from real experiments demonstrates the robustness of the proposed approach in material engineering as in (Halama et al., 2019) where a cyclic plasticity model was developed by ML starting from measures in the case of austenitic steel 08Ch18N10T. It also emerges that the idea of a stress-based memory surface applied to a virtual back-stress can also be used with other nonlinear kinematic hardening rules.
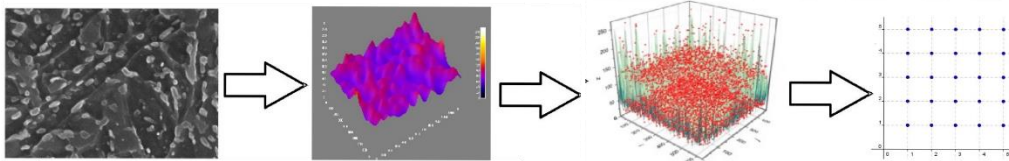
In brief, this paper shows how the concept of fractal geometry, powered by AI and ML, can be successfully applied to characterize metals microstructures deriving useful relationships between fractal dimensions and material features. Specifically, tool steel, hardened by laser and tested at room temperature for the indentation modulus was considered.

Therefore, a new approach for complexity determination by using fractals is proposed, validated by a direct application in analyzing microstructures. The achieved models enable to predict the mechanical properties of materials with respect to decisive parameters of laser beam and process. This study supports several others from authors (Babič et al., 2018; Fragassa, 2019, 2020).

2. MATERIALS AND METHODS

In this investigation, we used a robot laser cell RV60-40 (by *Reis Robotics*) for hardening conventional tool steel considering different parameters of speed $v \in [2, 5]$ mm/s and temperature $T \in [1000, 1400]$ °C.

A detailed characterization of the material microstructure before and after the surface treatment was done using the field emission scanning electron microscope (SEM), JEOL JSM-7600F. Then, those micrographs were digitalized for further analysis.

In particular, from the SEM 2D images (Figure 3a) and their levels of grey, we first rebuilt the profundity converting images into digital 3D (Figure 3b). With this scope, the *ImageJ* program (by National Institutes of Health) was used. After that, always continuing to benefit of *ImageJ* features, we identified the most representative points, able to outline and discretize the 3D profiles (Figure 3c). Finally, we extrapolated the (x,y,z) coordinates of points by perpendicular projection (Figure 3d).

Thanks to this method, the initial micrographs were converted in vectors and analysed.

Figure 3. Image processing methodology: from SEM images, passing by a 3D reconstruction of shapes, the definition of representative points, ending to the 2D projections.

The following analysis consisted in the determination of complexity passing by the fractals and the estimation of ***Hurst* exponent** (Yu et al., 2015).

With this scope, two options were available. As first, the *Hurst* exponent *(H)* in 3D space can be considered as the average space component of the diagonal linear graphs *xz* (Figure 3d). In this case, *Hurst* exponent *(H)* can be estimated using the sole *z* coordinates.

Those *z* coordinates are available in the 2D space by the component graph and are continuous. In addition, all the (x_i, y_0, z_i) points present first space component series in 2D graph for all (x_i, z_i). Simultaneously, all (x_i, y_1, z_i) present second space component in 2D graph for all (x_i, z_i). Thus, we evaluated the space component for all $(y_i, \forall_i)$. Then we estimated the *Hurst* exponent *(H)* for all these space components and, then, calculated the average of the *Hurst* exponent *(H)* for all these space components (Figure 4a) by equation (1):

$$H_{(x,z)}=(H_1+H_2+...+H_n)/n \qquad (1)$$

Secondly, we estimated the *Hurst* exponent *(H)* in the 3D space with the average space component of diagonal linear graphs. In this case, all (x_0, y_i, z_i) points represent first space component series in 2D graph for all *(yi, zi)*. All (x_1, y_i, z_i) points represent second space component in 2D graph for all *(yi, zi)*. We evaluated the space component for all $(x_i, \forall_i)$. Then, similarly to the previous case, we estimated the *Hurst* exponent *H* for all these space components and calculated the average of the *Hurst* exponent *H* for all these space components (Figure 4b) by equation (2).

$$H_{(y,z)}=(H_1+H_2+...+H_n)/n \qquad (2)$$

The fractal dimension was calculated by the following equation:

$$D=3- [H_{(y,z)}+ H_{(x,z)}]/2. \qquad (3)$$

For analysis of the results, several intelligent ***classificators***, namely a *Random Forest*, *Logistic Regression* and *Support Vector Machine* were used thanks to *Orange* open-source platform for machine learning.

$$H_{(x,z)} = \frac{H1 + H2 + ... + H15}{15}$$

$$H_{(y,z)} = \frac{H1 + H2 + ... + H15}{15}$$
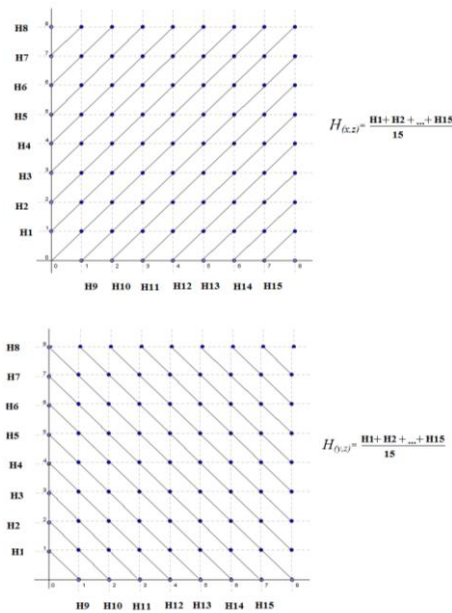
Figure 4. Complexity determination by using fractals and *Hurst* exponent (*H*)

2.1. The Random Forest method

The Random Forest method (RF) is an improvement in the *decision tree* technique, which consists in eliminating the correlation between the trees using a statistical method. As in the case of bagging, we build several hundred decision trees for training bootstrap samples. However, in each iteration of the tree construction, *m* is randomly selected from *p* predictors to be considered and the partition is allowed to be performed only for one of *m* variables. The meaning of this procedure, which turned out to be very effective for improving the quality of the obtained solutions, is that with the probability $(p − m) / p$ any potentially dominant predictor that seeks to enter every tree is blocked. If the dominance of such predictors is allowed, then all the trees will ultimately be very similar to each other, and the predictions obtained on their basis will strongly correlate and the decrease in variance will not be so obvious. By blocking dominants, other predictors will get their chance, and tree variation will increase (Figure 5).

Choosing a small value of *m* when constructing a random forest will usually be useful in the presence of many correlating predictors. Naturally, if a random forest is built using $m = p$, then the whole procedure is reduced to simple bagging.
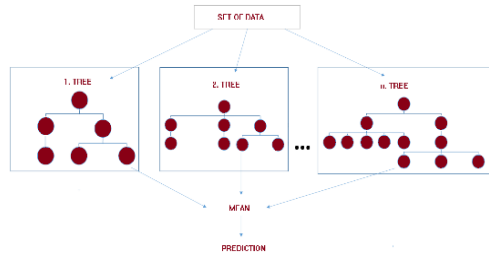
Figure 5. Random Forest

2.2. The k-Nearest Neighbors method

The closest similarity analysis, of which the k-Nearest Neighbors (kNN) represents a special application, is a general method for classifying observations based on the similarity of observations. This ML method has been developed as a way of recognizing data structures with the inaccurate matching of structures or observations. Similar observations are close to each other, and dissimilar observations, on the contrary, are removed from each other. Thus, the distance between two observations is a criterion for their difference. Close observations are also called "neighbors". When a new observation is presented, indicated by a question mark, its distance from all other observations in the model is calculated. The classification of the most similar observations (closest similarity) is determined and the new observation is placed in the category that contains the largest number of closest similarities. The user can specify the number of analyzed nearest neighbors; this value is denoted by k-nearby similarity (Campos et al., 2016) analysis can also be used to calculate values for a continuous target. In this situation, the average target value of the closest similarity is used to obtain the predicted value for the new observation (Figure 6).
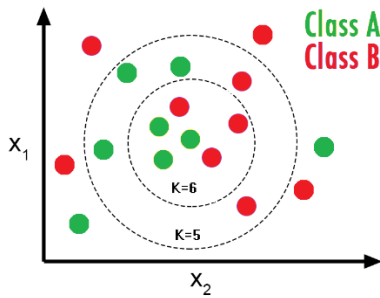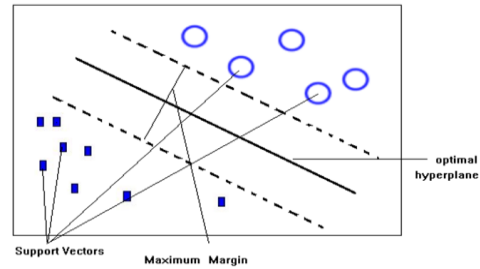
Figure 6. k-Nearest Neighbors

Figure 7. Support Vector Machine

2.3. The Support Vector Machine

The Support Vector Machine *(SVM)* method (Wenzel et al., 2017) uses a hyper-plane to classify data into 2 classes. A group of classification algorithms based on teaching with a teacher using a linear separation of objects in feature space using a hyperplane. The main idea of the method is the translation of the original vectors into a space of higher dimension and the search for a separating hyperplane with a maximum gap in this space. Two parallel hyperplanes are constructed on both sides of the hyperplane separating the classes. A separating hyperplane is a hyperplane that maximizes the distance to two parallel hyperplanes.

The algorithm works under the assumption that the greater the difference or distance between these parallel hyperplanes, the smaller the average error of the classifier.

The main problem of the method is the choice of the optimal hyperplane, which allows us to separate classes with maximum accuracy. For this, the separating hyperplane must be chosen so that the distance between the nearest points located on opposite sides of it is maximum. This distance is called the gap, and the points themselves are called reference vectors. Then the dividing hyperplane should be chosen in such a way as to maximize the gap, which will provide a more confident separation of classes (Figure 7).

3. Results and discussion

3.1. Experimental Measures

Table 1 shows data from N. 21 samples of laser hardened steel, reporting side-by-side process parameters, complexity indexes and materials properties. In particular, it displays the samples' values related to:

- laser beam **temperature**, in [°C]
- laser hardening **speed**, in [mm/s]
- **fractal dimension**, evaluated by the *Hurst* exponent
- surface **indentation** modulus*,* in [GPa], measured from experiments in accordance with ISO 14577.

For instance, sample *E18* after treatment of 1700 °C and 3 mm/s, shows the largest fractal dimension, 2.671, proof of the highest complexity in microstructure. Sample *E21,* on the other side, after treatment of 1850 °C and 2 mm/s shows the highest indentation modulus after hardening, equal to 230 GPa.

Those metal samples are reported in the table in the same order in which they were made.

In Figure 8 the graph line at the bottom displays values of beam temperature and speed for each sample clearly showing this sequence:

- laser beam temperature was progressively improved from 750 °C to 1850 °C in steps of 50 °C;
- for each step of temperature, a different hardening speed was used, cycling its value from 2 to 5 mm/s with steps of 1 mm/s.

The methodological choice to modify both parameters simultaneously allows to reduce the number of tests, but creates a complexity of the experimental conditions. By lacking a fixed base of comparison, it is not possible, for example, to observe the effect of each parameter when the other is kept fixed.

The use of artificial intelligence techniques makes it possible to overcome this limit thanks to their ability to recognize patterns on multiple levels.
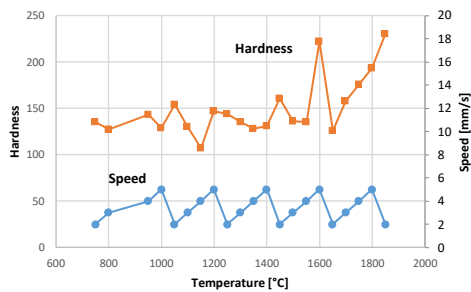
Figure 8. Changes in hardness and process speed for different laser beam temperatures

In the same figure, the upper line graph, displays the values of indentation modulus for each considered sample, with respect to the combination of beam temperature and speed. It is globally shown that hardness increases with beam temperature, especially in the presence of lower speed. At the same time, this effect is not so evident, and a deeper analysis is required before proving a result.

On the contrary, Figure 9 offers substantially consistent and definitive information. In this figure a comparison between the hardness moduli and the micrograph complexity, as measured by the *Hurst* exponent, for different laser beam temperatures and samples is reported. Line in the graphs are substantially overlapping in terms of trends (although the fact of having these different average values and ranges does not allow us to better assess this overlap). This confirms the approach chosen to use fractal geometry to interpret microstructures and the calculation of the Hurst exponent as a measure of fractal dimension.
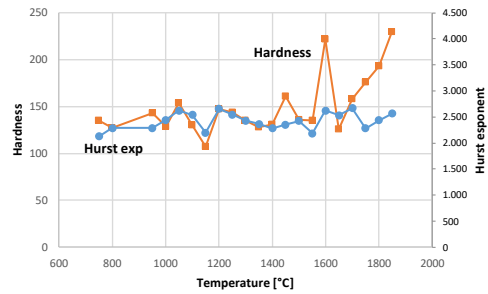
Figure 9. Comparison between hardness and micrograph complexity (as measured by the *Hurst* exponent) for different laser beam temperatures

3.2. Correlations

Linear correlations between these initial data were also investigated using the *Pearson* correlation coefficient. A linear correlation between two sets of data, (e.g. x_i and y_i) means that there is a direct proportionality between them. In this case, the *Pearson* correlation coefficient is close to 1 (or -1 for inverse proportionality), while coefficients close to 0 highlight uncorrelated data. At the same time, a relevant proportionality would be evident in graphs, too, since data, represented by (x_i, y_i) points, would be located quite close to the bisector.

Giving a new look to Figure 8, it is clear how temperature and speed (both parts of the experimental setup) are not related to each other, nor it was expected differently. It could be interesting, therefore, to evaluate the degree of correlation between the hardness and each of those variables. However, strong correlations are not to be expected, given that, as we said, hardness appears to be linked to a combination of both process parameters.
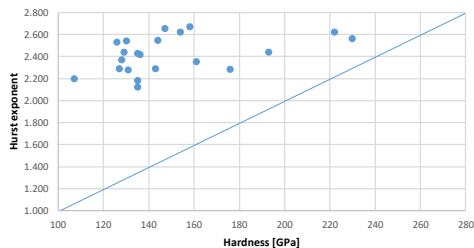
In terms of *Pearson* coefficients, temperature and hardness have 0.60 confirming a good direct linear correlation. The same level of correlation is not present in the case of temperature and *Hurst* exponent with a *Pearson* coefficients of 0.31 anticipating a certain dispersion of relationality in moving from experimental measurements to fractal geometry results.

Table 1. Parameters of hardened patterns

Sample	Temp	Speed	Hurst	Hardness
E1	750	2	2.124	135
E2	800	3	2.291	127
E3	950	4	2.288	143
E4	1000	5	2.441	129
E5	1050	2	2.622	154
E6	1100	3	2.541	130
E7	1150	4	2.198	107
E8	1200	5	2.654	147
E9	1250	2	2.547	144
E10	1300	3	2.429	135
E11	1350	4	2.368	128
E12	1400	5	2.281	131
E13	1450	2	2.354	161
E14	1500	3	2.421	136
E15	1550	4	2.183	135
E16	1600	5	2.624	222
E17	1650	2	2.531	126
E18	1700	3	2.671	158
E19	1750	4	2.283	176
E20	1800	5	2.438	193
E21	1850	2	2.565	230

Table 2. Experimental and prediction data

Sample	Hardness	RF	SVM	k-NN
E1	135	131	144	137
E2	127	147	144	137
E3	143	125	141	132
E4	129	138	144	137
E5	154	162	135	128
E6	130	137	143	133
E7	107	133	134	137
E8	147	138	144	133
E9	144	136	135	139
E10	135	135	135	130
E11	128	136	135	140
E12	131	130	143	154
E13	161	136	143	154
E14	136	147	135	154
E15	135	149	134	160
E16	222	133	145	147
E17	126	176	145	165
E18	158	141	144	172
E19	176	168	136	181
E20	193	180	135	161
E21	230	220	135	176

In the case of speed and hardness the *Pearson* coefficient is -0.09 showing an extremely weak inverse relation. This inversion was also noted in the previous section.

Regarding the two data sets shown in Figure 9, where a comparison between hardness and micrograph complexity was provided, a *Pearson* coefficient, equal to 0.42, highlights a medium strong correlation between them. This is also represented in Figure 10 with points distributed in ascent but far from the bisector

Figure 10. Relation between hardness and complexity, as measured by *Hurst* exponent

3.3. Data prediction

Data from Table 1, as said, were used to train different ML algorithms. By a *supervised* ML approach, the AI was requested to find recurrences and patterns in the full set of data (21x4). Then, three different intelligent algorithms, specifically, *Random Forest* (RF)*, Support Vector Machine* (SVM) and *k-Nearest Neighbors* (kNN) proposed their own values for the hardness. Predictions and measures are reported in Table 2.

Figure 11 also displays the values giving the opportunity for a visual comparison between experiments and predictions. It is shown, in particular, that all methods predict the measure with a good level of accuracy in the central part of the range (115-145 GPa). Instead, they tend to lose precision immediately when experimental data moves away from the more frequent values. The only exception is RF which shows better flexibility.

M. Babič, C. Fragassa, G. Lesiuk, D. Marinković
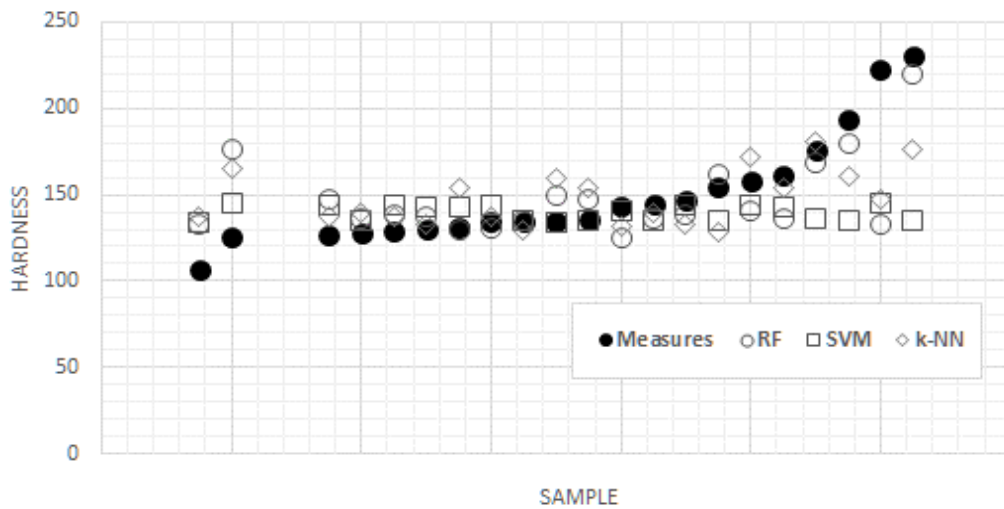
Figure 11. Experimental measures and predicted values by *Random Forest* (RF), *Support Vector Machine* (SVM) and *k-Nearest Neighbors* (kNN) methods

3.4. Prediction accuracy

The accuracy of predictions was evaluated by
- *Pearson Correlation Coeffic.* (PCC)
- *Mean Relative Error* (MRE)

Both of those numeric procedures can help judge the goodness of fit. While the first one is mainly concerned, as already said, with evaluating the linearity between the two data sets, the second deals only with evaluating the average difference between the values. Their results are reported in Table 3.

Table 3. Accuracy of prediction methods

Methods	RF	SVM	k-NN
PCC	0.58	-0.06	0.50
MRE	11.69%	15.63%	13.18%

Regarding the *MRE* evaluation, in particular, the RF model gives 11,69%, representing the highest value of accuracy in prediction indentation modulus of robot laser hardened samples, followed by 13.18% in the case of *k-NN* and 15.63% for SVM.

Considering the *PCC* evaluation, with a linear coefficient of -0.06, the SVM predictor is also confirmed as inappropriate with respect to which the remaining two should be preferred. Furthermore, with a *PCC* of 0.58, also in this case the RF method offers better correlation respect to k-NN where *PCC* is 0.50.

4. Summary

The main findings and outcomes of the current research can be summarized as:
1. a method, based on fractal geometry, able to analyse the microstructure of metals and alloys was developed, validated and used with success.
2. microstructures were identified from micrographs, rebuilding their three-dimensionality, before converted them in fractals by evaluation of specific features (*Hurst* exponent).
3. microstructures were related to material properties thanks to experimental tests performed in accordance with standards;
4. between the other properties, micro-indentation was preferred considering its relevance in representing the effect of hardening;
5. process and experimental data, coming from 21 samples, were used to train specific machine learning algorithms, chosen between many others considering previous researches and experiences;

6. experimental indentation values were predicted with an appreciable accuracy (with mean error ~10%);

7. among them, the *random forest* and *k-nearest neighbors* offered a good level of usability and have to be preferred compared to the *support vector machine.*

5. Conclusions

In conclusion, the paper presented a new method for the determination of structural complexity of materials by using fractal geometry and applies this method to the surface characterisation of tool steel, thermally treated by laser hardening.

High-performance and high-quality processes for metal hardening can be successfully implemented today by using robot laser hardening technology.

At the same time, the optimisation of process parameters, often necessary, can be arranged using the emerging techniques of machine learning. They permit to recognize patterns and recurrences in metal microstructures and relate them with the mechanical properties.

With this scope, fractal geometry can be usefully merged in the method. Fractals, in fact, can convert micrograph structures into formulas without losing relevant information on their peculiarity. It is also the way for transferring this kind of information inside a mathematic framework for further analyses.

For the purpose, a machine learning approach is perfect due to the capability to perform the pattern recognition at a multilevel.

Passing by three *classificators* (as *Random Forest*, *Support Vector Machine* and *k-Nearest Neighbours*) was introduced in the present case. Available in an open-source platform, they were used for searching recurrences between process parameters and experiments data.

In particular, micro-indentation was chosen as key experimental property to be focused on due to its relevance in monitoring the process quality in the case of laser hardening.

In the future, the question on how to improve the validity in prediction can be related to: using another method of intelligent systems, make optimization of robot laser parameters or enlarging the dataset adopted for training.

References:

Babič, M., Calì, M., Nazarenko, I., Fragassa, C., Ekinovic, S., Mihaliková, M., ... & Belič, I. (2019). Surface Roughness Evaluation in Hardened Materials by Pattern Recognition Using Network Theory. *International Journal on Interactive Design and Manufacturing*, *13*(1), 211-219. doi: 10.1007/s12008-018-0507-3

Babu, P. D., Buvanashekaran, G., & Balasubramanian, K. R. (2012). Experimental studies on the microstructure and hardness of laser transformation hardening of low alloy steel. *Transactions of the Canadian Society for Mechanical Engineering*, *36*, 242-257. doi: 10.1139/tcsme-2012-0018

Bashir, S., Vaheed, H. and Mahmood, K. (2013). Nanosecond Pulsed Laser Ablation of Brass in a Dry and Liquid-Confined Environment. *Applied Physics*, *A110*, 389-395

Bishop, C. M. (2006). *Pattern Recognition and Machine Learning*. Springer

Campos, G. O., Zimek, A., Sander, J., & Ricardo, J. (2016). On the evaluation of unsupervised outlier detection: measures, datasets, and an empirical study. *Data Mining and Knowledge Discovery*. *30*(4), 891-927. doi:10.1007/s10618-015-0444-8

Chiang, K. A., & Chen, Y. C. (2005). Laser surface hardening of H13 steel in the melt case. *Material Letters*, *59*(14-15), 1919-1923

Choi, S. G., Hwang, I., Kim, Y. M., Kang, B., & Kang, M. (2019). Prediction of the Weld Qualities Using Surface Appearance Image in Resistance Spot Welding. *Metals*, *9*(8), no. 831. doi:10.3390/met9080831

Fragassa, C., Babic, M., Bergmann, C. P., & Minak, G. (2019) Predicting the tensile behaviour of cast alloys by a pattern recognition analysis on experimental data. *Metals*, *9*, 557. doi:10.3390/met9050557

Fragassa, C., Babic, M., Pavlovic, A., & do Santos, E. D. (2020). Machine Learning Approaches to Predict the Hardness of Cast Iron. *Tribology in Industry.* doi: 10.24874/ti.2020.42.01.01

Halama, R., Fumfera, J., Gál, P., Kumar, T., & Markopoulos, A. (2019). Modeling the Strain-Range Dependent Cyclic Hardening of SS304 and 08Ch18N10T Stainless Steel with a Memory Surface. *Metals*, *9*(8), no. 832. doi:10.3390/met9080832.

Kazakevich, P. V., Simakin, A. V., Shafeev, G. A., Monteverde, F., & Wautelet, M. (2007). Phase Diagrams of Laser-Processed Nanoparticles of Brass. *Applied Surface Science*, *253*, 7724-7728.

Koch, H. V. (1904). Sur une courbe continue sans tangente, obtenue par une construction géométrique élémentaire. *Arkiv for Matematik, Astronomi och Fysik*, *1*, 681-704.

Kotowski, P. (2006). Fractal dimension of metallic fracture surface. *International Journal of Fracture*, *141*(1-2), 269-286.

Kotowski, P., Lesiuk, G., Correia, J. A., & de Jesus, A. M. (2018, November). Mixed mode (I+II) fatigue crack paths in S355J0 steel in terms of fractal geometry. *AIP Conference Proceedings*, *2028*(1), 020005. AIP Publishing.

Lin, Z.Z.P., & Ren, L. (2014) The Mechanical Properties and Microstructures of AZ91D Magnesium Alloy Processed by Selective Laser Cladding with Al Powder. *Optics and Laser Technology*, *60*, 61-68

Majumdar J. D., Manna I., Kumar A., Bhargava P., & Nath A. (2009). Direct laser cladding of Co on Ti–6Al–4V with a compositionally graded interface. *Journal Material Processing Technology*, *209*, 2237-2243. doi: 10.1016/j.jmatprotec.2008.05.017

Mandelbrot, B. B. (1975). *Fractals: form, chance, and dimension* (Vol. 706). San Francisco: WH Freeman

Mandelbrot, B. B. (1983). *The fractal geometry of nature* (Vol. 173, p. 51). New York: WH freeman.

Mandelbrot, B. B., Passoja, D. E., & Paullay, A. J. (1984). Fractal character of fracture surfaces of metals. *Nature*, 308(5961), 721-722.

Martin, J. D. (2015). What's in a Name Change? Solid State Physics, Condensed Matter Physics, and Materials Science. *Physics in Perspective*, *17*(1), 3–32. doi:10.1007/s00016-014-0151-7

Michael I. J. (2014). *Statistics and machine learning*. Reddit. Retrieved 2014-10-01.

Naeem, S., Mehmood, T., Wu, K. M., et al. (2019). Laser Surface Hardening of Gun Metal Alloys. *Materials 12*(16), 2632. doi: 10.3390/ma12162632

Ostwald, M. J., & Vaughan, J. (2016). *The Fractal Dimension of Architecture*. Birhauser, Basel. doi:10.1007/978-3-319-32426-5.

Pande, C. S., Richards, L. E., Louat, N., Dempsey, B. D., & Schwoeble, A. J. (1987). Fractal characterization of fractured surfaces. *Acta Metallurgica*, *35*(7), 1633-1637.

Pang, J., Zhou, Z., Zhao, Z., Tang, D., Liang, J., & He, Q. (2019). Tensile Behavior and Deformation Mechanism of Fe-Mn-Al-C Low Density Steel with High Strength and High Plasticity. *Metals*, *9*(8), no. 897. doi:10.3390/met9080897

Smith, D. R., Padilla, W. J., Vier, D. C., Nemat-Nasser, S. C., & Schultz, S. (2000). Composite Medium with Simultaneously Negative Permeability and Permittivity (PDF). *Physical Review Letters*, *84*(18), 4184.

Wenzel, F., Galy-Fajou, T., Deutsch, M., & Kloft, M. (2017). Bayesian Nonlinear Support Vector Machines for Big Data. Machine Learning and Knowledge Discovery in Databases (ECML PKDD). *Lecture Notes in Computer Science, 10534*, 307-322. doi:10.1007/978-3-319-71249-9_19

Yu, S., Piao, X., Hong, J., & Park, N. (2015). Bloch-like waves in random-walk potentials based on supersymmetry. *Nature Communications*, *6*, 8269.

Zhang, H, Yang X., Cui, H, & Wen, W. (2019). Study on the Effect of Laser Quenching on Fretting Fatigue Life. *Metals*, 9(5), no. 566. doi:10.3390/met9050566

Matej Babič
Faculty of Information
Science in Novo Mesto,
Novo Mesto, Slovenia,
babicster@gmail.com

Cristiano Fragassa
Alma Mater Studiorum
University of Bologna
Bologna, Italy
cristiano.fragassa@unibo.it

Grzegorz Lesiuk
Wroclaw University of
Science and Technology,
Wrocław; Poland
grzegorz.lesiuk@
pwr.edu.pl

Dragan Marinković
Technical University Berlin
Berlin, Germany
dragan.marinkovic@
tu-berlin.de